International Journal of Mechanical, Industrial and Aerospace Sciences
ISSN: 2517-9950
Vol:8, No:9, 2014

Optimisation of a Dragonfly-Inspired Flapping Wing-Actuation System

Jia-Ming Kok, Javaan Chahl

Abstract—An optimisation method using both global and local optimisation is implemented to determine the flapping profile which will produce the most lift for an experimental wing-actuation system. The optimisation method is tested using a numerical quasi-steady analysis. Results of an optimised flapping profile show a 20% increase in lift generated as compared to flapping profiles obtained by high speed cinematography of a *Sympetrum frequens* dragonfly. Initial optimisation procedures showed 3166 objective function evaluations. The global optimisation parameters - initial sample size and stage one sample size, were altered to reduce the number of function evaluations. Altering the stage one sample size had no significant effect. It was found that reducing the initial sample size to 400 would allow a reduction in computational effort to approximately 1500 function evaluations without compromising the global solvers ability to locate potential minima. To further reduce the optimisation effort required, we increase the local solver's convergence tolerance criterion. An increase in the tolerance from 0.02N to 0.05N decreased the number of function evaluations by another 20%. However, this potentially reduces the maximum obtainable lift by up to 0.025N.

Keywords—Flapping wing, Optimisation, Quasi-steady model.

I. Introduction

In recent years, Unmanned Aerial Vehicles (UAVs) have been a growing area of research. Since the inception of UAVs, these unmanned aircraft have begun replacing piloted aircraft particularly in Defence applications. Their operational uses include aerial surveillance and reconnaissance and support to ground forces.

One particular branch of UAV research has been focussed on biologically inspired flapping wing aircraft. This area of research has been facilitated by technological advancements in many fields including micro-electronics, sensors, microelectromechanical systems, and micro-manufacturing. Bio-inspired flapping wing aircraft differ from conventional fixed and rotary wing aircraft in that they offer benefits including increased efficiency at low Reynolds numbers making them a viable design for small size, low speed aircraft, otherwise known as Micro Air Vehicles (MAVs) [1], [2]. In addition, flapping wing flyers cover a large range of strategic manoeuvres not singularly capable by their fixed or rotary wing counterparts. Dragonflies in particular are one of the most amazing flyers. The dragonfly planform was one of the first to evolve and is thus amongst the longest surviving flying organisms. Its ancestry can be traced back to the *Protodonata*, which are amongst the earliest winged insect fossils discovered [3], [4]. The evolution and optimization of the dragonfly planform dates back 300 million years.

This evolutionary process has made dragonflies extremely versatile flyers. Dragonflies demonstrate an aerial agility that allows it to out manoeuvre and prey on other insects. Slow motion footage taken by Ruppell [5] show instantaneous accelerations of up to 4g and sustained and take-off accelerations of up to 2g. Maximum speeds demonstrated by dragonflies were up to 10m/s which are in the order of the operational speeds of some MAVs. Analysis of a video of dragonflies in combat by Chahl et al. [6] showed accelerations in turns exceeding 4g. Wind tunnel studies performed by Alexander [7] show that at low speeds, dragonflies employ a "yaw turn" manoeuvre whereby a 90^o yaw is achieved in 2 wing beats. It is these properties that allow for sophisticated predation strategems [8] that make dragonflies excellent aerial predators. In addition to being extremely manoeuvrable, dragonflies are able to sustain prolonged periods of hover. Like many other insects, the dragonfly has evolved a flapping wing-actuation system that allows it to overcome the large cyclic forces required for hovering flight. The extensive capabilities of the dragonfly can be attributed to the unique degree of control the dragonfly has over its flapping actuators and hence flapping profile [9], [10]. Alexander showed through high speed cinematography in a wind tunnel [7] the capability of the dragonfly to adjust both its stroke plane angle and angle of attack of the individual wings to perform complex yawing or banking turns. Even during hovering flight, Wang [11] proposed that dragonflies rely on adjusting the angle of attack of the wing to reduce the energy costs of hover. Certainly observations of the wing actuators of dragonflies support these theories. An investigation of the actuation system in dragonflies shows their capability to actively control and effect wing rotation [9], [12]. These factors highlight the importance of wing articulation and the flapping profile in dragonfly flight.

This paper will present a dragonfly-inspired wing-actuation system design and the methods used to tune the flapping-wing profile to produce optimal performance for that wing-actuation system.

II. Wing-Actuation System

To replicate the flight capabilities of the Dragonfly, a fully controllable, 3 Degrees-of-Freedom (DOF) wing-actuation system is proposed that accurately represents the key characteristics of the dragonfly wing-actuation system. To date we have built a test bench prototype (see Fig. 1) of

Jia-Ming Kok is with the School of Engineering, University of South Australia, Mawson Lakes, Australia (phone: +61424610329; e-mail:jia.kok@mymail.unisa.edu.au).

Javaan Chahl is the Chair of Sensor Systems at the University of South Australia, Mawson Lakes, Australia (e- mail:javaan.chahl@unisa.edu.au).

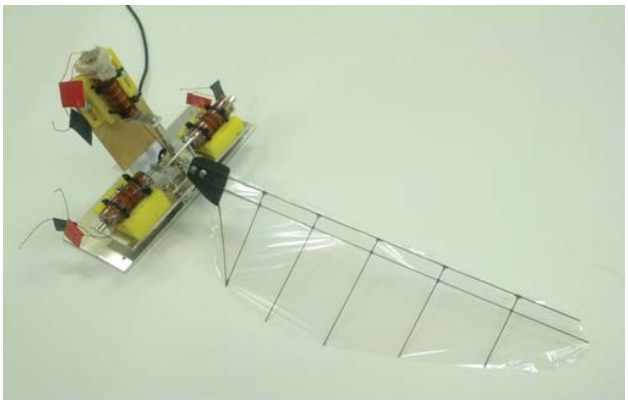

Fig. 1. Fully software controllable, 3DOF flapping wing-actuation system

the wing-actuation system using custom-built solenoids as the main form of actuation. Solenoids were selected as their linear motion more closely represents the system of muscles in a Dragonfly. Three solenoid actuators are used to allow the wing-actuation system to articulate the wing in 3 DOF similar to in the Dragonfly. A direct drive mechanism for transferring solenoid displacement to wing displacement was employed. Complex indirect mechanisms can be utilised, however anatomical studies have shown that the Dragonfly uses a direct drive mechanism whereby the actuators are attached directly to the root of the wing [13]. A force/torque transducer is used to measure the forces generated by the wing-actuation system.

The design of the wing was based on a dragonfly wing profile. Initial wings were designed with a 7cm span, however preliminary experiments showed significant levels of noise being generated. Therefore, a larger 30cm wing design was selected, operating at lower wing-beat frequencies. The larger wing allows for larger aerodynamic forces to be generated, while the lower wing-beat frequencies would reduce the overall noise and loads in the system, hence improving the signal-to-noise ratio. The wing was constructed from Mylar skin, overlaid over a carbon fibre rod-spar structure. The final design is shown in Fig. 1.

Following the design of a wing-actuation system, it is necessary to determine the flapping wing profile which will produce the most lift during hover. High speed cinematography of dragonflies in hover shows that the optimal flapping profile varies between different dragonflies [14], [15], [16]. This suggests that the optimal flapping profile is highly system specific, and therefore requires the use of optimisation methods to determine the wing profile.

III. Optimisation Problem

Both computational and experimental methods can be used to optimise the flapping profile. Berman and Wang [17] used blade element theory analysis to minimise the power requirements of their prescribed flapping profile whilst maintaining sufficient lift for three different insects. Ghommem et al. [18] used a modified blade element theory analysis to obtain maximum lift generation. Thomson et al. [19] used experimental methods to determine the optimal flapping profile for a scaled-up moth (Manduca Sexta) wing.

Regardless of the method, all the optimisation techniques share a common issue. The non-linear flapping-wing dynamics leads to multiple optima across the response surfaces, and depending on the initial solution the obtained local optima might not correspond to the global optima. That is particularly true for the problem of flapping wing actuation. To resolve this issue, optimisation techniques that rely on global search methods will have to be used.

To do this, we employ a Global Search algorithm presented by Ugray et al. [20]. This is a combination of global and local search methods for finding multiple local optima. Global methods are used to determine basins where optima are likely to occur, and local gradient-based methods are used to refine the location of the optima within those basins. An initial set of points are produced by using a Scatter Search approach [21]. Similar to Genetic algorithms, this is a heuristic approach. However, unlike genetic algorithms that require a large initial populations to generate sample points, the Scatter Search approach uses a small initial set of samples and grows the sample size based on not just the value of the objective function, but also the diversity of that solution. Therefore, the Scatter Search method produces a set of sample points that both satisfy the objective function but are sufficiently diverse from each other that the probability of locating the true global optima is increased. Once an initial population of sample points have been determined, local Quasi-Newton optimisation techniques [22], [23] are employed to refine the location of the optima to within a user-specified convergence criterion. The objective function being optimised is the lift generated by the wing-actuation system.

A. Quasi-steady Model

To tune the parameters of the optimisation routine and demonstrate its functionality, a numerical quasi-steady blade element model of the aerodynamic forces acting on the flapping wing was produced. Similar studies have been performed by Weis-Fogh, Norberg [24], [25]. Sane and Dickinson [26] also presented a similar analysis, with additional aerodynamic effects due to wing rotation. The wing was divided into spanwise sections, and the instantaneous forces calculated on each section based on the local translational and angular velocity. The forces across all slices were then summed to obtain the forces/torques acting on the wing at any point in time.

The wing kinematics were represented using equations from Berman and Wang [17], [27], [28] for a wing flapping in an inclined stroke plane with angle β. This inclined stroke plane is more characteristic of a dragonfly flapping profile. The flapping angle, ϕ, and angle-of-attack, α, in the stroke plane is represented by

$$\phi(t) = \frac{\phi_m}{sin^{-1}(K))} sin^{-1}[Kcos(\omega t)] \quad (1)$$

$$\alpha(t) = \frac{\alpha_m}{tanhC_\alpha} tanh[C_\alpha cos(\omega t + \Phi_\alpha)] + \alpha_0 \quad (2)$$

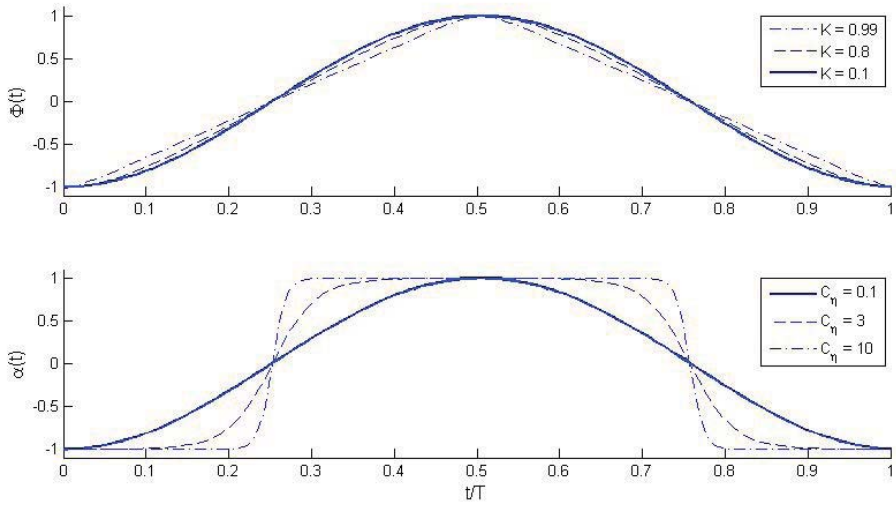

Fig. 2. Illustration of the dependance of ϕ and α on K and C_η (adapted from Berman and Wang [17]).

where $0 < K < 1$ and $C_\eta > 0$. In the limit where $K \to 0$, ϕ becomes sinusoidal, and in the limit where $K \to 1$, a triangular waveform is generated. Similarly, as $C_\eta \to 0$, α becomes a sinusoidal waveform, as $C_\eta \to \infty$, α tends towards a square wave (refer to Fig. 2).

To determine if such a model is able to represent the key characteristics of the flapping wing profile, we compare the output of this model against known experimental results obtained by high speed cinematography of a *Sympetrum frequens* dragonfly undertaken by Azuma et al. [15].The flapping and pitch angles at 20 different locations along the wing path were measured. A Fourier series expansion was performed to fit a continuous curve with the experimental results. The curve-fitted experimental results shows that the flapping profile, $\phi(t)$ is approximated by a sinusoid and hence

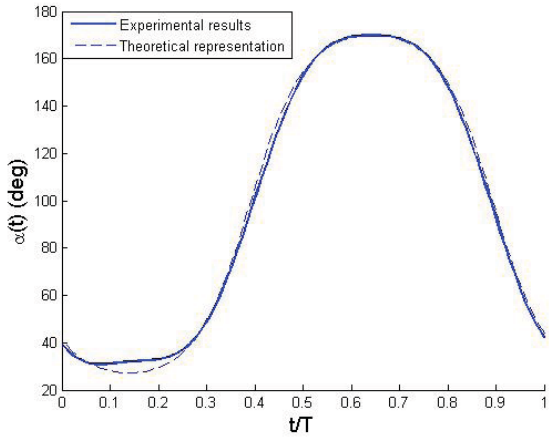

Fig. 3. A comparison of the periodic hyperbolic function proposed by Berman and Wang [17] (dashed line) with experimental results from Azuma et al.[15] (solid line)

Berman and Wang's representation for the flapping angle (refer to (1)) is appropriate. The curve fitted experimental results for the pitch angle, $\alpha(t)$, have components of a second and third harmonic and hence cannot be represented by a sinusoidal profile. However, a comparison of the experimental pitch angles with the periodic hyperbolic function suggested by Berman and Wang (refer to (2)) shows that the periodic hyperbolic function is able to approximate the wing pitch profile (refer to Fig. 3). Additionally, the periodic hyperbolic function is fully defined by 4 variables as opposed to the 7 variables required by a triple harmonic Fourier series representation.

Once the flapping and pitch profile have been determined, the local velocity at each spanwise section of the wing as well as the lift and drag coefficients can be determined, and used to calculate the forces due to the translational (refer to Fig. 4) and rotational (refer to Fig. 5) motion of the wing.

Equations for the lift and drag coefficients were obtained from three-dimensional experiments performed by Dickinson [27], [29]. Similar coefficients were obtained by Wang computationally and used as the basis for analysing dragonfly flight [27], [28]. Morphological parameters for the wing shape were obtained from Norberg [30].

$$V = r\dot{\phi} \tag{3}$$

$$C_L = 0.225 + 1.58sin(2.13\alpha - 7.2) \tag{4}$$

$$C_D = 1.92 - 1.55cos(2.04\alpha - 9.82) \tag{5}$$

The aerodynamic forces were then calculated at each section of the wing.

$$dL = 0.5\rho V^2 C_L dS \tag{6}$$

$$dD = 0.5\rho V^2 C_D dS \tag{7}$$

Similarly, the rotational pressure forces for each section of the wing were modelled as

$$C_{rot} = \pi(0.75 - \hat{x_0}) \tag{8}$$

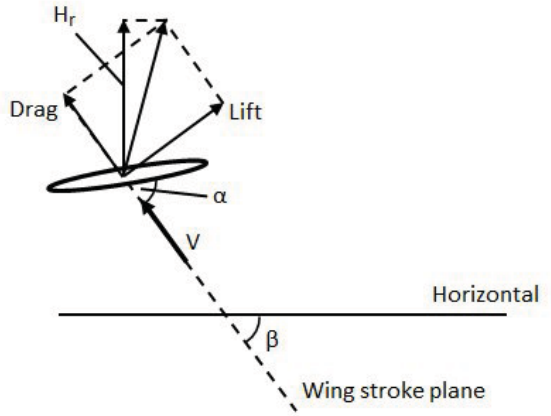

Fig. 4. Illustration of the aerodynamic forces acting on a single section of the wing.

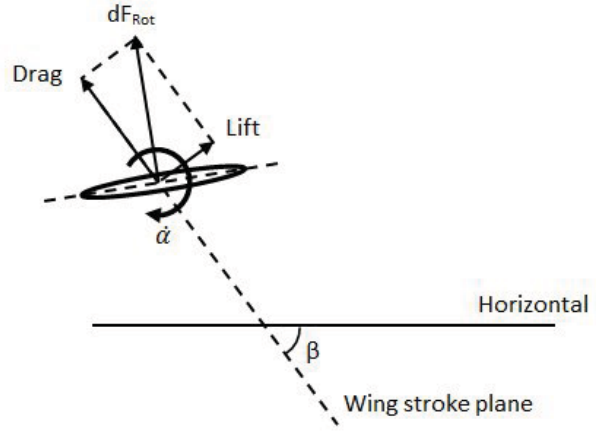

Fig. 5. Illustration of the pressure force due to rotational circulation acting on a single section of the wing.

$$dF_{rot} = C_{rot}\rho c^2 U\dot{\alpha}dr \tag{9}$$

where $\hat{x_0}$ is the non-dimensional axis of rotation from the leading edge. The overall aerodynamic force can then be calculated by summing the force of all wing sections. It should be noted that the direction of the lift and drag forces are with respect to the velocity of the wing section. To determine the actual lift force generated by the wing in the global reference frame, a coordinate transformation was employed (refer to Fig. 6). The vertical force in the frame of reference of the wing is given by (10).

$$H_r = Lcos(\beta) + Dsin(\beta) + F_{rot}sin(\alpha - \beta) \tag{10}$$

The vertical force with respect to the global frame of reference is

$$H_{r,vert} = H_r cos(\phi_{Proj}) \tag{11}$$

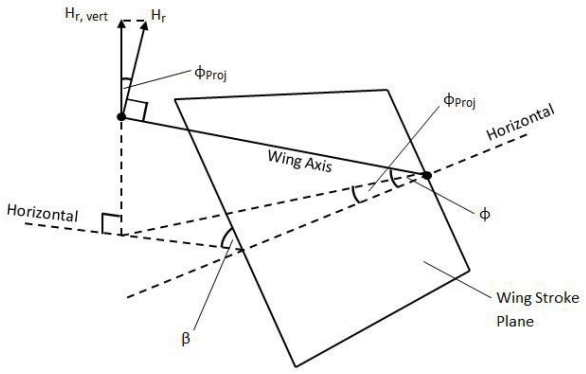

Fig. 6. Illustration of the coordinate transform required to determine the actual lift generated by the wing in the global frame of reference (adapted from Norberg [25]).

An equation for $cos(\phi_{Proj})$ was calculated using the formulation from Norberg [25]. Therefore the vertical force with respect to the global frame of reference is

$$H_{r,vert} = H_r\sqrt{1 - sin^2\alpha sin^2\beta} \tag{12}$$

With a method of calculating the objective function now defined, the optimisation problem can be expressed as:

$$X = [\beta, K, \overset{min}{C_\eta}, \Phi_\alpha, \alpha_0, \alpha_m] \qquad -H_{r,vert} \tag{13}$$

subject to the following optimisation restrictions

$$X_{i,min} \leq X_i \leq X_{i,max} \qquad \forall i \in \{1,2,3,4,5,6\} \tag{14}$$

and constraints

$$\alpha_m - \alpha_0 \leq -10^o \tag{15}$$

$$\alpha_m + \alpha_0 \leq 170^o \tag{16}$$

These restrictions are selected to constrain the solution space within the limits of the physical test bench design illustrated in Fig. 1. Additionally, C_η was constrained, to limit the maximum angular pitch velocity of the system. The constraints are given in Table I

TABLE I
OPTIMISATION CONSTRAINTS

Property	Lower Limit	Upper Limit
β (deg)	10	80
K	0.1	0.99
C_η	0.1	1.3
Φ_α (deg)	0	-180
α_η (deg)	10	90
α_0 (deg)	40	140

IV. Results

Prior to running the optimisation process, the lift generated was calculated for the flapping profile suggested by Azuma et al.[15]. Previously we determined that Berman and Wang's [17] representation of the flapping and pitch profile was sufficient to represent the experimental results obtained through high speed cinematography by Azuma et al (refer to Fig. 3). The values used to approximate the experimental flapping and pitch curves are as follows:

TABLE II
Initial optimisation parameters

Property	Value
β (deg)	37.0
K	0.1
C_η	1.3
Φ_α (deg)	-49.0
α_η (deg)	70.8
α_0 (deg)	99.1

The wing-beat frequency for the *Sympetrum frequens* dragonfly quoted by Azuma et al was 41.5Hz, which is not achievable by our flapping wing system. Therefore the wing-beat frequency was capped at 10Hz. A quasi-steady numerical analysis was performed on that flapping profile, and the mean lift obtained was 0.55N. The optimisation algorithm was run to determine the flapping profile which would produce the most lift.The Scatter Search algorithm, working from the initial flapping profile, produced a population consisting of a 1000 members which was filtered to 200 'Stage One' members. Local Quasi-newton methods were then used to refine the solution and determine the optimal flapping profile. Fig. 7 shows the optimised flapping and pitch profile versus the unoptimised profile. The lift profiles across the wing stroke for both the optimised and initial cases are shown in Fig. 8. The final optimised parameters were:

TABLE III
Optimised flapping profile parameters

Property	Value
β (deg)	10.0
K	0.1
C_η	1.3
Φ_α (deg)	-63.6
α_η (deg)	56.1
α_0 (deg)	94.5

Results of the quasi-steady analysis showed that the mean lift over the wing stroke increased to 0.67N from 0.55N initially. This corresponds to an increase of 22%. However, this was achieved after 3166 objective function evaluations. Whilst this is appropriate for computer simulations, it is not ideal for an experimental optimisation. The reason for this is the finite time required to experimentally measure the lift associated with each sample. Additionally, the progressive wear associated with running the experimental wing-actuation system for extended periods of time could result in changes to the system being optimised. Therefore, the number of objective function evaluations will have to be reduced in order for the optimisation algorithm to be applicable to experimental conditions.

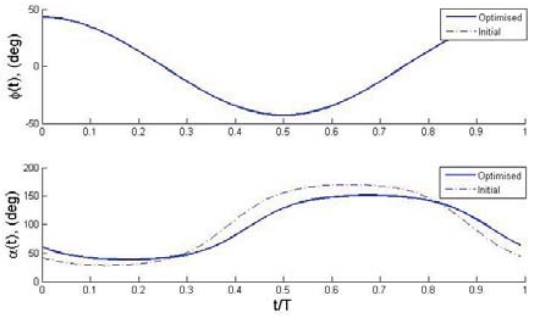

Fig. 7. Optimised flapping profile (solid lines) versus unoptimised flapping profile (dashed lines)

As mentioned previously, the global Scatter Search algorithm generates a population of a 1000 initial trial points initially from which it then selects 200 of the best points to perform a local Quasi-Newton optimisation. Minimise the initial number of trial points reduces the number of function evaluations required. However, this comes at the risk of potentially missing the global optimum. To investigate this effect, we progressively reduce the number of initial sample points and measure the optimised lift. Due to the random nature of the scatter search algorithm, we execute the optimisation algorithm 10 times for each point of interest to ensure consistency in the results. Fig. 9 shows the change in the number of objective function evaluations required with a change in the initial number of trial points used. The error bars represent the scatter in the results obtained from the optimisation method. When the initial population size is reduced to 200, there is reduction in the number of function evaluations to an average of 481. However, it was observed

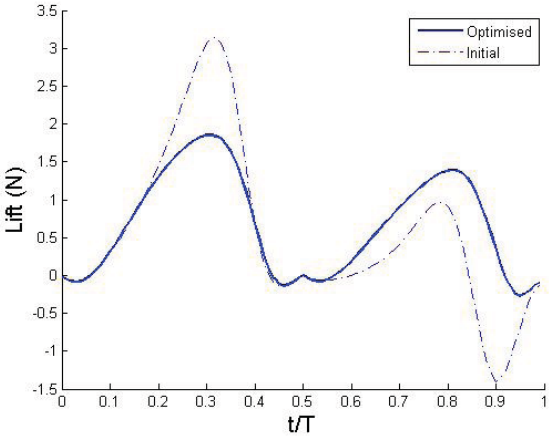

Fig. 8. Optimised lift profile (solid lines) versus unoptimised lift profile (dashed lines)

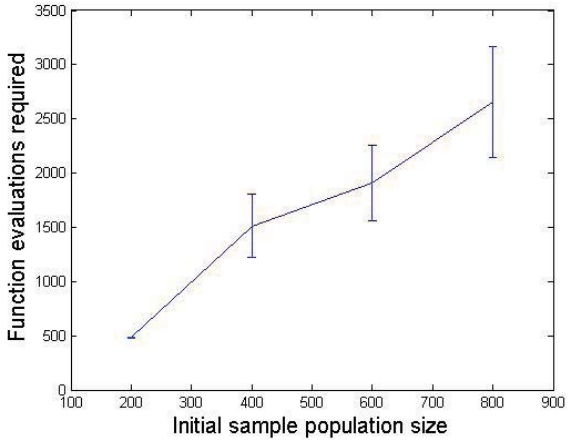

Fig. 9. Number of function evaluations required versus initial population size

that there was a variation in the lift generated between 0.65 to 0.67N, even though the objective function convergence tolerance was set to 0.01N. This suggests that using 200 initial samples is not sufficient to consistently capture the global optima. Therefore, an initial population size of 400 will be used.

We next investigate the effect of reducing the number of 'Stage 1' samples (refer to Fig. 10). As shown, there is no significant change in the number of function evaluations required with a change in Stage one sample size.

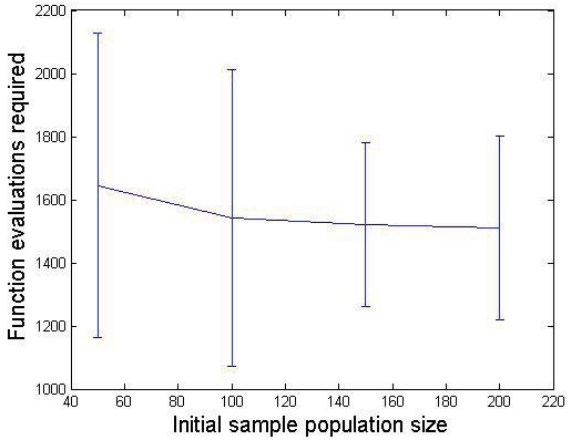

Fig. 10. Number of function evaluations required versus Stage One population size

Adjusting the number of initial trial points and 'Stage one' points both affect the global optimisation process. It is also possible to reduce the number of function evaluations by adjusting the convergence tolerance of the local, Quasi-newton optimisation algorithm. As shown in Fig. 11, there is a clear decrease in the number of function evaluations required by approximately 20% when the tolerance size is increased to 0.05N from 0.02N. There is no significant change with further tolerance increase above 0.05N.

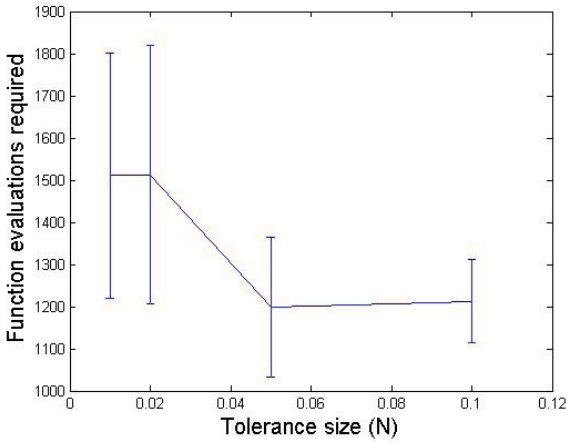

Fig. 11. Number of function evaluations required versus the tolerance of the local solver

Increasing the tolerance of the convergence criterion comes at the cost of the ability of the local optimiser to refine the optimised solution. As shown in Fig. 12, the optimised lift averages 0.65N for a tolerance size of 0.05N as opposed to 0.67N for a tolerance size of 0.01N. At 0.1N tolerance, the scatter in the lift obtained becomes too large, suggesting a solver with inconsistent performance.

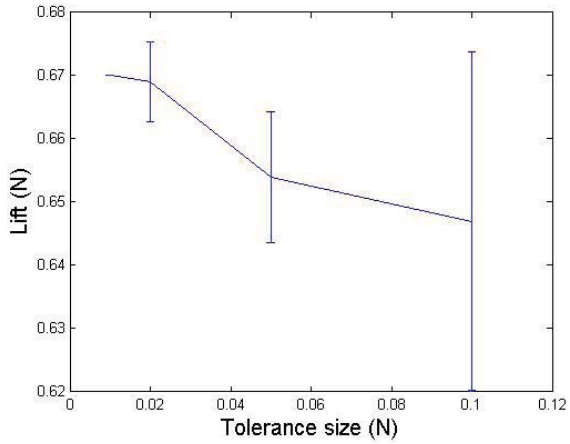

Fig. 12. Lift forces generated by the optimisation algorithm as a function of the convergence tolerance criteria.

V. Discussion

A quasi-steady blade element model was generated to investigate the functionality of a combined global and local optimisation algorithm. Results showed a 20% increase in lift between the optimised and unoptimised flapping profile. It was found that by reducing the initial sample size from 1000 to 400, and increasing the convergence tolerance criterion to 0.05N, significant reductions in the number of function evaluations could be achieved.

Reductions in the number of function evaluations is critical to an experimental wing-actuation system optimisation. Using a tolerance of 0.05N was found to decrease the lift by up to 4%, however this could be insignificant in comparison to the variation in lift due to the noise generated by an experimental test bench. Results from an optimisation by Thomson et al. [19] showed the significance of noise in an experimental set-up. The noise was sufficiently large that using an iteration step size of 5^o produced no convergence. Increasing the iteration step size of the local solver is another factor which will potentially allow reductions in the number of function evaluations. However, this could also result in a reduction in the precision of the solution.

In section III-A we discussed the adaptation of Berman and Wang's methodology to representing the flapping and pitch profile of a dragonfly. By comparison with experimental results, we demonstrated that Berman and Wang's model is able to model the flapping profile of a real world dragonfly with reasonable accuracy. Whilst it is possible to use a Fourier expansion with second and third harmonics to better model the flapping profile, it also introduces additional parameters which need to be optimised and hence the optimisation effort required. This was done by Thomson et al.[19]. However, their results showed that an iterative step of 10^o was required in order to achieve convergence, which raises the question as to the benefits of having the additional precision of a Fourier expansion in a real world system.

Further work will focus on implementing the optimisation algorithm on the experimental wing-actuation system. Initial efforts would be targeted at maximising lift, however other objective functions would be investigated, including maximum lift-to-power and maximum yaw moment.

VI. Conclusion

The nature of the flapping wing problem is such that the flapping wing profile is unique to each system. Therefore, optimisation methods are required in order to determine the flapping profile which will deliver optimal performance. However, flapping wing systems are characterised by non-linear dynamics that produces multiple optima across its response surface. In this paper, we present an optimisation method using both global and local optimisation to determine the flapping profile which will produce the most lift for an experimental wing-actuation system. The optimisation method is first tested using a numerical quasi-steady analysis to determine the functionality of the optimisation algorithm. Results of an optimised flapping profile show a 20% increase in lift generated as compared to flapping profiles obtained by high speed cinematograhy of a *Sympetrum frequens* dragonfly. An initially untuned optimisation algorithm showed that the objective function was evaluated 3166 times which is not suitable for an experimental setup. Initial sample size and stage one sample size, were altered to determine its effect on the number of function evaluations. Whilst the stage one sample size had no significant effect on reducing the optimisation effort, reducing the initial sample size reduced the number of function evaluations significantly. It was found that reducing the initial sample size to 400 would allow a reduction in computational effort to approximately 1500 function evaluations without compromising the global solvers ability to determine the locations of potential minima. To further reduce the optimisation effort required, we increase the local solver's convergence tolerance criterion. An increase in the tolerance from 0.02N to 0.05N decreased the number of function evaluations by another 20%. However, this potentially reduces the maximum obtainable lift by up to 0.025N. In summary, using a quasi-steady numerical analysis we have demonstrated the ability of the optimisation algorithm to converge on an optimised flapping wing solution in $\tilde{1}200$ function evaluations to within 0.025N accuracy.

References

[1] S. Ashley, "Palm-size spy plane," *Mechanical Engineering*, vol. 120, no. 2, pp. 1–11, 1998.
[2] J. Sirohi, "Microflyers: inspiration from nature," in *SPIE Smart Structures and Materials+ Nondestructive Evaluation and Health Monitoring*. International Society for Optics and Photonics, 2013, pp. 86 860U–86 860U–15.
[3] R. Wootton, "The fossil record and insect flight," in *Symp. R. Entomol. Soc. Lond*, vol. 7, 1976, pp. 235–254.
[4] M. L. May, "Heat exchange and endothermy in protodonata," *Evolution*, pp. 1051–1058, 1982.
[5] G. Rüppell, "Kinematic analysis of symmetrical flight manoeuvres of odonata," *Journal of Experimental Biology*, vol. 144, no. 1, pp. 13–42, 1989.
[6] J. Chahl, G. Dorrington, and A. Mizutani, "The dragonfly flight envelope and its application to micro uav research and development," in *AIAC15: 15th Australian International Aerospace Congress*. Australian International Aerospace Congress, p. 278.
[7] D. E. Alexander, "Wind tunnel studies of turns by flying dragonflies," *Journal of Experimental Biology*, vol. 122, no. 1, pp. 81–98, 1986.
[8] A. Mizutani, J. S. Chahl, and M. V. Srinivasan, "Insect behaviour: Motion camouflage in dragonflies," *Nature*, vol. 423, no. 6940, pp. 604–604, 2003.
[9] Sviderskiĭ, "Structural-functional peculiarities of wing appatatus of insects that have and do not have maneuver flight]."
[10] J. M. Kok and J. Chahl, "Resonance versus aerodynamics for energy savings in agile natural flyers," in *SPIE Smart Structures and Materials+ Nondestructive Evaluation and Health Monitoring*. International Society for Optics and Photonics, 2014, pp. 905 504–905 504.
[11] Z. J. Wang, "Dissecting insect flight," *Annu. Rev. Fluid Mech.*, vol. 37, pp. 183–210, 2005.
[12] P. Simmons, "The neuronal control of dragonfly flight. i. anatomy," *The Journal of Experimental Biology*, vol. 71, no. 1, pp. 123–140, 1977.
[13] R. Dudley, *The biomechanics of insect flight: form, function, evolution*. Princeton University Press, 2002.
[14] A. Azuma and T. Watanabe, "Flight performance of a dragonfly," *Journal of Experimental Biology*, vol. 137, no. 1, pp. 221–252, 1988.
[15] A. Azuma, S. Azuma, I. Watanabe, and T. Furuta, "Flight mechanics of a dragonfly," *Journal of experimental biology*, vol. 116, no. 1, pp. 79–107, 1985.
[16] J. Wakeling and C. P. Ellington, "Dragonfly flight. i. gliding flight and steady-state aerodynamic forces," *Journal of Experimental Biology*, vol. 200, no. 3, pp. 543–556, 1997.
[17] G. J. Berman and Z. Wang, "Energy-minimizing kinematics in hovering insect flight," *Journal of Fluid Mechanics*, vol. 582, pp. 153–168, 2007.
[18] M. Ghommem, M. R. Hajj, L. T. Watson, D. T. Mook, R. Snyder, and P. S. Beran, "Deterministic global optimization of flapping wing motion for micro air vehicles," in *Proceedings of the 13th AIAA/ISSMO Multidisciplinary Analysis Optimization Conference, AIAA Paper*, no. 2006-1852, 2010.
[19] S. L. Thomson, C. A. Mattson, M. B. Colton, S. P. Harston, D. C. Carlson, and M. Cutler, "Experiment-based optimization of flapping wing kinematics," in *Proceedings of the 47th Aerospace sciences meeting*, 2009.
[20] Z. Ugray, L. Lasdon, J. Plummer, F. Glover, J. Kelly, and R. Martí, "Scatter search and local nlp solvers: A multistart framework for global optimization," *INFORMS Journal on Computing*, vol. 19, no. 3, pp. 328–340, 2007.

[21] F. Glover, M. Laguna, and R. Martí, "Fundamentals of scatter search and path relinking," *Control and cybernetics*, vol. 39, no. 3, pp. 653–684, 2000.
[22] P. E. Gill, W. Murray, M. A. Saunders, and M. H. Wright, "Procedures for optimization problems with a mixture of bounds and general linear constraints," *ACM Transactions on Mathematical Software (TOMS)*, vol. 10, no. 3, pp. 282–298, 1984.
[23] P. Gill, W. Murray, and M. Wright, "Numerical linear algebra and optimization vol. 1, 1991."
[24] T. Weis-Fogh, "Quick estimates of flight fitness in hovering animals, including novel mechanisms for lift production," *Journal of Experimental Biology*, vol. 59, no. 1, pp. 169–230, 1973.
[25] R. A. Norberg, "Hovering flight of the dragonfly aeschna juncea l., kinematics and aerodynamics," *Swimming and flying in nature*, vol. 2, pp. 763–781, 1975.
[26] S. P. Sane and M. H. Dickinson, "The aerodynamic effects of wing rotation and a revised quasi-steady model of flapping flight," *Journal of Experimental Biology*, vol. 205, no. 8, pp. 1087–1096, 2002.
[27] Z. J. Wang, J. M. Birch, and M. H. Dickinson, "Unsteady forces and flows in low reynolds number hovering flight: two-dimensional computations vs robotic wing experiments," *Journal of Experimental Biology*, vol. 207, no. 3, pp. 449–460, 2004.
[28] Z. J. Wang, "The role of drag in insect hovering," *Journal of Experimental Biology*, vol. 207, no. 23, pp. 4147–4155, 2004.
[29] M. H. Dickinson, F.-O. Lehmann, and S. P. Sane, "Wing rotation and the aerodynamic basis of insect flight," *Science*, vol. 284, no. 5422, pp. 1954–1960, 1999.
[30] R. k. Norberg, "The pterostigma of insect wings an inertial regulator of wing pitch," *Journal of comparative physiology*, vol. 81, no. 1, pp. 9–22, 1972.